Satellite Imagery Analysis of Ice Edge Eddy Dynamics

Andrew Mather Cowan, Scott Polar Research Inst., University of Cambridge, Lensfield Road, Cambridge CB2 1 ER, England, UK,

Klaus Alfred Ulbricht (co-chairman of WG 7, oceanography and coastal zone), Institut für Optoelektronik, German Aerospace Research Establishment (DFVLR), 8031 Wessling, FR Germany.

Commission No. VII, Working Group 7

Introduction

The observation and study of ocean current variability as revealed by eddies has always been problematic due to the space and time scales involved. Satellite remote sensing has improved this position enabling oceanographers to obtain synoptic time series observations where there are indications of such phenomena. While surface temperature variations may serve as indicators, detected by infrared observation, other tracers may have equal value when atmospheric conditions or a lack of surface temperature information render infrared measurements unreliable. For example, Ulbricht et al. (1978 a, b, 1983) have indicated the feasability of monitoring blue-green algal surface distributions in the Baltic. Sea ice is another tracer of particular importance, for it dominates the oceans in data-sparse areas and it masks other surface indicators such as water temperature.

The marginal ice zone (MIZ) may be defined as that zone of the ice cover which is subject to the direct effect of open ocean conditions, typically up to 100 km from the ice edge. The ice cover of the Arctic Ocean may be modelled as a continuum with marco-scale constitutive properties and bounded by a semicontinuous coastline. The MIZ is not amenable to such treatment, it is bounded on one side by a solid constraint, i.e. a coastline and, possibly, a variable depth of non-MIZ ice cover, the other boundary being a thermal front with the warmer surface water of the open sea. The ice cover of the MIZ is not a continuum, for it is constantly being fractured by incident wave energy and other mechanisms into floes, varying in diameter from a few meters to tens of kilometers, The MIZ ice has greater freedom of movement and is acted upon by internal stress fields, winds, currents, and wave radiation pressure, which together control the morphology of the ice edge. The East Greenland Current (EGC) is a classic example of an MIZ, and the dynamics of its ice edge are the subject of a long term research project at the Scott Polar Research Institute. The existence of eddies in the EGC is of great importance as a factor in heat and mass balance, for each eddy at the edge of the ice cover temporarily disrupts the Polar Front, and allows the exchange of heat, salt and nutrients between the Greenland Sea and polar waters. The EGC is a region of intense flow, and NOAA-6, 7 and 8 and LANDSAT-2, 3 images, collected in a near continuous dataset from May 1981 to the present, reveal in the ice cover the complex meandering and advective vortices characteristic of such regions.

One aspect of the dynamics of the ice edge is that of the mesoscale (10-50 km diameter) Vortices at the ice margin. These strip away the outermost few kilometers of floes and either mix them in the warmer water beyond the Polar Front or fold them back into the main body of the ice cover, producing a banded structure of alternating large and small floes. Each band is a reflection of the floe size distribution in the region of the ice edge prior to the action of the vortex, and may be from hundreds of meters to several kilometers in width.

The scale and morphology of such eddies may indicate the forcing mechanism. It is certainly likely that the small scale features (< 10 km diameter) are wind generated, possibly by atmospheric roll vortices (Muench and Charnell, 1977). It is possible, that the mesoscale features are also wind-generated, for example, caused by the ice responding to the passage of a storm track, where the wind shifts through a large arc. However, there is strong evidence, that this scale of feature in the ice cover is indeed a tracer of an oceanographic process. Vinje (1977) detected in LANDSAT imagery a cyclonic vortex at the ice margin in the Fram Strait, having a diameter of approximately 50 km. This observation was supported by a Nimbus-6 satellite tracked buoy, indicating a circulating surface feature. Since that time a further twelve definite identifications of this apparently near stationary vortex (77° - 79° 30'N, 00°E) have been made from satellite imagery. Supporting evidence came from submarine velocity profiles obtained in 1976 in the same area which had revealed a structure of warm Atlantic Intermediate Water bands within the Polar Front (Wadhams et al., 1979). In 1980, during the cruise of the Swedish icebreaker YMER, the area was investigated and a vortex was observed in the expected position. It was demonstrated to be oceanographic and not simply a surface wind-generated feature. The enclosed warm water lenses found within the Polar Water Correlated with zones of reduced ice concentration (Wadhams and Squire, 1983). Such a relationship between ice concentration and water temperature may be of general use in identifiying such features in satellite imagery. In a general sense, eddies in a region of intense flow are produced by eddy-mean field interactions. These are large amplitude processes, related in a strong horizontally sheared current to baroclinic instability or to combined baroclinic and barotropic processes (Robinson, 1983).

Current interaction with changes in bottom topography and instabilities in frontal regions are also recognized causative mechanisms. Wadhams and Squire (1983) explained the Fram Strait feature as a case of a buoyancy driven vortex along a front, but did suggest that its spatial stationarity near the Molloy Deep, a 5770 m circular ocean floor hole at 79°10'N, 2°50'E, may be significant. This latter suggestion was supported by Morrison et al. (1983), and bathymetric generation was argued in opposition to an explanation in terms of the density structure of the ocean. Morrison et al. argued that it was not simply a case of the Molloy Deep in isolation, but rather a complex of deeps and mounts in the area, that generate the eddy.

In the SPRI EGC ice edge study a second near stationary eddy system has been observed in the Denmark Strait between Iceland and Greenland. The Denmark Strait is the outlet gap for the ice and waters of the EGC into the North Atlantic (Figure 1).

Antropova et al. (1980) calculated that the average velocity of the EGC at 66°N in May and April is 220 km/month, the average width of the current is 130 km and the area of ice transported across the line of latitude is 29000 km² per month. The current velocity rises rapidly at the current boundary (Einarsson, 1972). A current of warmer Atlantic water flows north on the Iceland side of the Strait.

On the Greenland side of the Strait the coastal shelf extends in a projection at 400 m depth to near the center of the Strait. On the Iceland side the coastal shelf extends similarly with a predominant depth of 200 meters. A narrow channel of 600 meters maximum depth, 60 km width and 200 km north-east to south-west extension, thus constricts the flow of deep water from the relatively deep waters to the north (depth 1600 m maximum), and the deep Atlantic, 150 km to the south (depth 2600 m). Smith (1976) demonstrated, that the overflow through the Strait pulsed at a regular period during a month's observation; the spectral peak was shown to be 1.8 days.

The earliest satellite imagery observation of the Denmark Strait eddy system in the context of this study, was July 1978. A diffuse ice edge with a series of cyclonic gyres of approximately 20 km diameter was observed over the northern end of the narrow channel. In May 1980 a compact gyre approximately 80 km in diameter was observed in a similar position. These observations led to the systematic monitoring of imagery of the area, starting in May 1981. Due to cloud cover it has been difficult to establish long time series observations. Indeed the longest series yet collected for any section of the ice edge is sixteen days. A detailed study of the dynamics of the Denmark Strait ice cover must therefore be based on a number of years of satellite observations. In order to pursue such a detailed study, optimum methods of NOAA and LANDSAT image processing and analysis are being developed. LANDSAT satellites are equipped with multispectral scanners (MSS), which register different spectral appearances of the Earth periodically from a height of roughly 900 km. Scanning is accomplished in the cross-track direction by an oscillating mirror, where six lines are scanned simultaneously in each of four spectral bands for each mirror sweep. The forward motion of the satellite provides the along-track progression of the scan lines. The sensor system responds to the reflection of sunlight from the Earth in the four spectral bands MSS4 to MSS7, 0.5 - 0.6 µm, 0.6 - 0.7 µm, 0.7 - 0.8 µm, and 0.8 - 1.1 µm.

Two LANDSAT 2 images of the Denmark Strait eddy system have been studied in detail, for they represent the 'diffuse' and 'compact' cases of the same system, as observed in 1978 and 1980. The first image from April 23, 1981, here designated Eddy-A, shows the diffuse case. The central point of the image is at 66° 25'N 24° 47'W. MSS 7, the near IR channel, detects radiation which is reflected from the surface of the water, and provides the greatest amount of information on the structure of the ice cover, i.e. in terms of discerning discrete floes within the matrix of brash and small floes. However, there is some loss of detail at diffuse sections of the ice edge. MSS 4, the shorter wavelength channel from 0.5 to 0.6 µm, detects solar radiation reflected from suspended material to a depth of 3 - 5 meters, and provides the most detail of the structure of the ice edge where it is composed of a diffuse cover of brash ice. A combination of channels 4, 5, and 7 was found to provide the best compromise in terms of a single image for interpretation (Fig. 2).

The shape of the vortex as viewed in Figures 2 and 3 indicates an overall anticyclonic motion on a scale of approximately 200 km N-S extension. Ice edge protrusions and the infolding of ice bands indicate local cyclonic motion. In the interior of the feature a marked vortex street exhibiting cyclonic and anticyclonic gyres on an average scale of approximately 10 km may be seen on the left of the images.

Meteorological data from meteorological data point 1 at 66°00'N 30°00'W (Fig. 1) show, that on April 23 the Denmark Strait was at the southern edge of a Greenland high pressure area. Consequently an east-north-easterly was blowing in the area of Eddy-A with a strength varying between 4 and 15 knots. The last storm system to have moved SE-NE through the Strait was on April 15 and therefore is irrelevant.

Grey scale stretching of a LANDSAT image* has been used to examine the detail of the interior circulation and morphology of the feature (Figure 4a) Inclusions of open water are clearly seen and the size distribution of floes can be measured. In Fig. 3 the floe size distribution is a negative exponential with a maximum floe diameter of 20.8 km. In Fig. 2 the number of large floes has been drastically reduced with the largest flow diameter being 9,7 km. However, the most significant aspect of the change in floe size distribution is the drastic reduction in floes of all sizes to create on ice cover almost completely composed of brash and cakes (i.e. < 20 m diameter). The process of advecting the floes out of the main body of the ice cover through the action of the vortex exposes them to accelerated fracture by wave action and enhanced melting within the mixed surface water of the vortex. The drastic alteration in the floe size distribution occurs within a short distance. Fig. 4b shows a small section of the top edge of Fig. 2. In the top left hand corner of this figure can be seen a compact zone of floe size distribution and ice concentration characteristic of the interior ice cover as found just to the north (Fig. 3). South of this point the mixing of surface waters has destroyed all traces of this zone except for a trail of relatively large floes nearer to the ice edge. Fig. 4c is a stretched image of the southerly section of the small scale vortex street. That it is etched out on the ocean surface in an ice cover entirely composed of brash ice, may be clearly seen. The dimensions of the gyres and the overall morphology of this vortex are further enhanced in a pseudoplastic image (Fig. 4d). As a point of interest Von Karman's model of vortex streets assumed flow to be nonviscous and 'initially' laminar. He found that for a street to remain stable the ratio between vortex width and distance between vortices was 0.28. The viscosity of ocean surface water with an ice cover leads one to expect a higher ratio. An average ratio of 0.6 was found for the presently observed vortex street.

* Image processing was done at DIBIAS, the image processing facility of the German Aerospace Research Establishment (DFVLR), Oberpfaffenhofen.

The scale of the vortices making up the vortex street indicates a meteorological process. The wind, blowing over the ice cover composed of relatively large floes, may interact with the convective currents over the northern end of the bight of open water and brash ice created by the eddy, in a manner similar to air flow encountering a solid body. The diffuse southern edge of Eddy-A is also explained by the prevailing winds.

Similar indications of processes acting upon the ice cover may be observed in the MSS 7 image of Eddy-B (Fig. 6). The central point of this image is at 66°23'N and 24°52'W. This image, from 11 May 81, shows the compact case of the vortex, also having an anticyclonic motion and being approximately 92 km in N-S extension. Here again, protrusions and infolded bands at the seaward ice edge indicate local cyclonic motion, probably caused by a combination of prevailing winds and waves.
Meteorological data from meteorological data point 2 at 68°00'N and 25°00'W (Fig. 1) show, that south-south-westerly winds of 22-27 knots increasing were blowing. Storm conditions had prevailed since the previous day.
The internal structure of Eddy-B was clarified using a grey-scale streched MSS 7 image (Fig. 8), and a section of this image (Fig. 8b) clearly shows the floes and the brash and cake matrix. The floe size distribution exhibited in Fig. 7 is again a negative exponential with a maximum floe diameter of 26 km. In Eddy-A the floe size distribution has been radically altered within the body of the vortex in terms of maximum size and range. A maximum floe diameter of 17 km is found at the northern edge of the eddy, while further south the largest floe is 6.5 km in diameter. Again the exposure of floes to warm water intrusions and enhanced wave fracturing appears to be the process at work. Fig. 8c shows ice banding on the seaward side. In Fig. 8a the southern edge of Eddy-B is seen to be compact and this is obviously due to the prevailing winds. However, in Fig. 8d, an MSS 4 grey-scale stretched image structure may be seen beyond the ice edge. Give the characteristics of MSS 4 radiation detection, it would seem that this image detects the very diffuse cover of small ice fragments often to be found beyond the ice edge.

It is clear, that many of the small scale features of these eddy systems can be explained in meteorological terms. However, the location of Eddy-A over the northern end of the narrow Denmark Strait bathymetric gap and the junction of the strong southerly flowing EGC and the warmer northward flowing current of Iceland suggests the predominance of oceanographic effects in its formation. Further evidence for this was found in NOAA-6 IR imagery, which shows the relative temperature differences of surface waters outside and within the eddies.

Summary

This analysis indicates that the detailed study of satellite imagery can yield useful information on the processes acting within and upon ice eddies. Given significant time series of synoptic image data sets, and supporting meteorological and oceanographic data, eddy dynamics in polar regions may be better understood.

References:

Antropova, L.V., et al. (1980). A calculation of the basic components of ice balance in the Denmark Strait, US Army Corps of Engineers Cold Regions Research and Engineering Laboratory (CRREL), Draft Transl. 742

Einarsson, T. (1972), Sea currents, ice drift and ice composition in the East Greenland Current, in Sea Ice, T. Karlsson, ed., Nat. Res. Counc. of Iceland, Reykjavik, 23-32

Morison, J.et al. (1983) Comment on 'An ice-water vortex at the eddy of the East Greenland Current' by Wadhams and Squire, submitted to J.Geophys.Res.

Muench, R.D. and Charnell, R.L. (1977), Observation of mediumscale features along the seasonal ice edge in the Bering sea, J.Phys.Oceanogr. 7 (4), 602-606

Robinson, A.R., (1983), Overview and summary of eddy science, ch. 1 of Eddies in Marine Science, Springer Verlag

Smith, P.C. (1976), Baroclinic instability in the Denmark Strait overflow, JPO 6: 355-371

Ulbricht, K.A. Schmidt, D., Horstmann, U. (1978a) 'Mass Appearance of Blue-Green Algae in the Baltic Sea: Evaluation of Multispectral LANDSAT Scenes by Image Processing', Proceedings of an International conference on Earth Observation from Space and Management of Planetary Resources, Toulouse, France (ESA SP-134), 77-79

Ulbricht, K.A.,Horstmann, U., Schmidt, D., (1978b) 'Detection of Eutrophication Phenomena from Air and Space', Proceedings of the Twelfth International Symposium on Remote Sensing of Environment, Manila, Philippines, 1379-1389

Ulbricht, K.A., (1983), 'LANDSAT image of Blue-Green Algae in the Baltic Int. J. Remote Sensing, Vol.4, No. 4, 801-802

Vinje, T.E., (1978). On the use of data buoys in sea ice studies, presented at WMO Workshop on Remote Sensing of Sea Ice., Wash., DC, 16-20 Oct.78

Wadhams, P., Gill, A.E., Linden, P.F. (1979), Transects by submarine of the East Greenland Polar Front, Deep Sea Res. 26, 1311-1327

Wadhams, P., Squire, V.A. (1983). An ice-water vortex at the edge of the East Greenland Current, J.Geophys. Res., 88 (5), 2770-2780

Figures

Fig.1 Chart of Denmark Strait showing position of Eddies A+B and positions of meteorological data points
Fig.2 Eddy A, combination of MSS 4, 5, and 7 (false colour representation)
Fig.3 MSS 7 Quick-look image of ice conditions in LANDSAT, frame location immediately north of Eddy A
Fig.4 Eddy A, MSS 7, grey level stretched to enhance internal structure of vortex
(b) Part of (a) enhanced, to point out discrete floes
(c) MSS 7 grey level streched to enhance vortex street
(d) MSS 4, pseudoplastic image of vortex street
Fig.5 Eddy B, NOAA-6 image showing geographical context
Fig.6 Eddy B, MSS 7 of LANDSAT scene
Fig.7 MSS 7 Quick-look image of ice conditions in LANDSAT frame location immediately north of Eddy B
Fig.8 (a) Eddy B, MSS 7, gray level stretched to enhance internal structure of vortex
(b) section of MSS 7 showing internal detail of vortex
(c) section of MSS 7 showing banding at ice edge
(d) MSS 4 revealing greater minor detail at ice edge

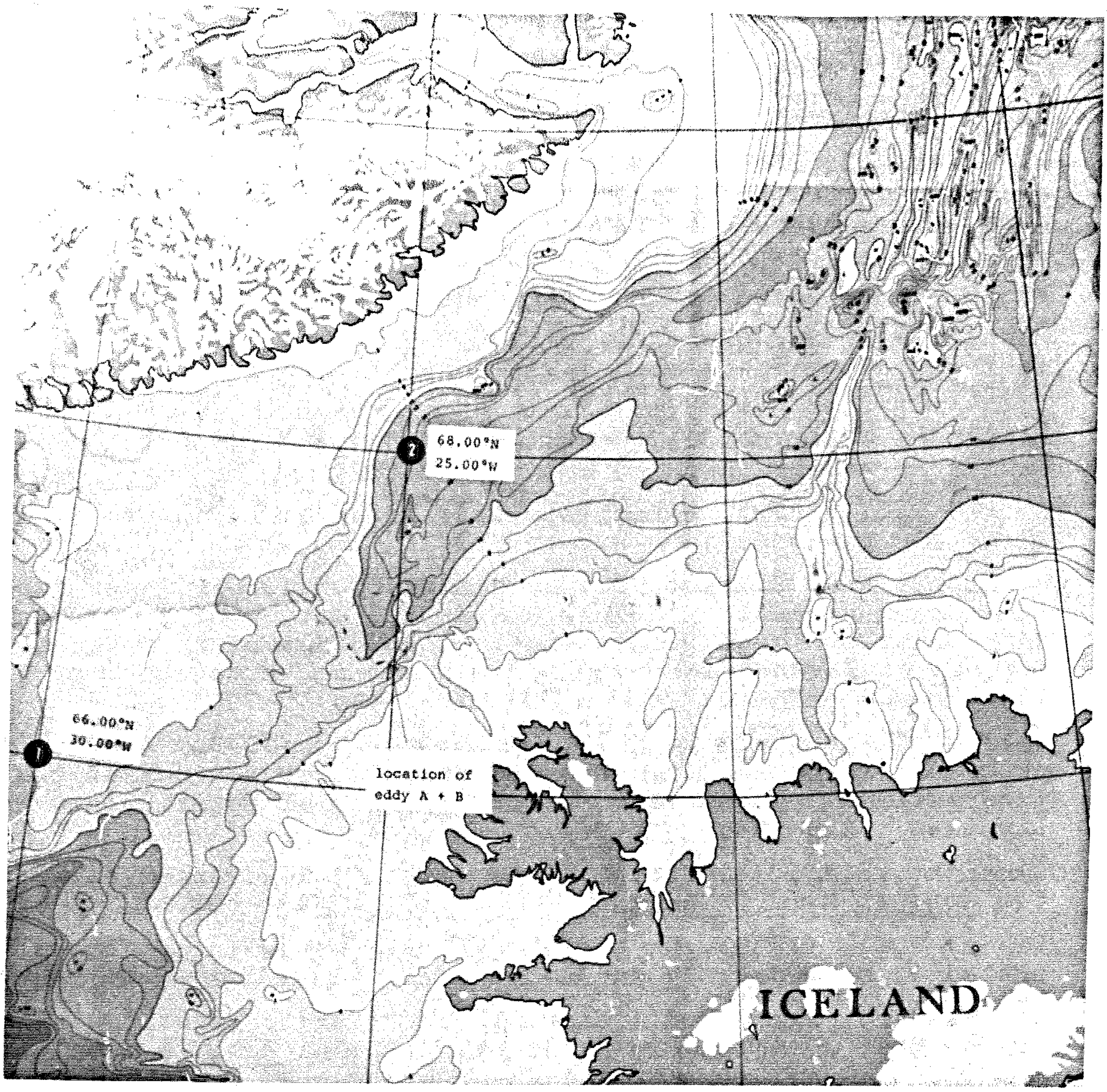

FIG. 1

FIG. 2

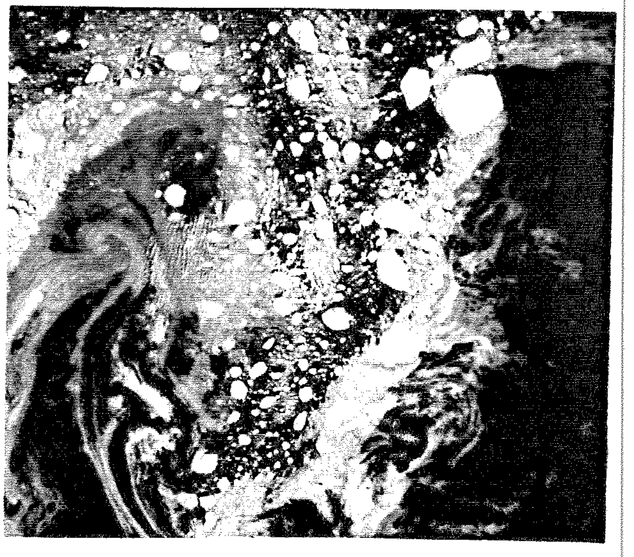

FIG. 3

FIG. 4a

FIG. 4b

FIG. 4c

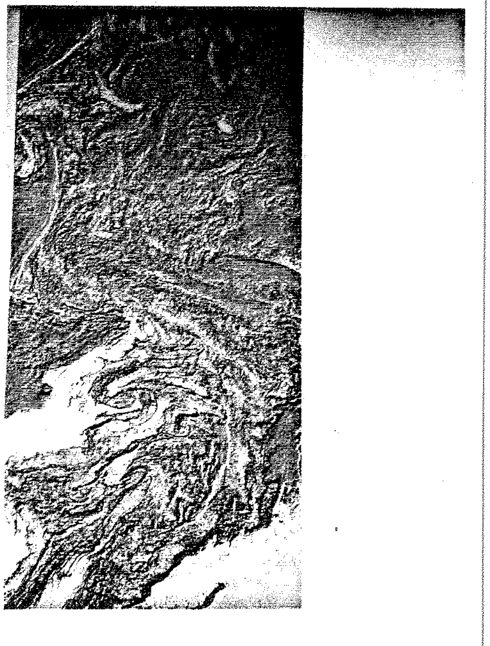

FIG. 4d

FIG. 5

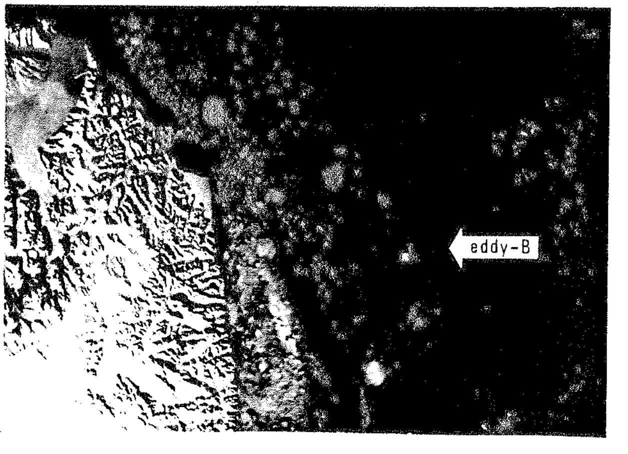

FIG. 6

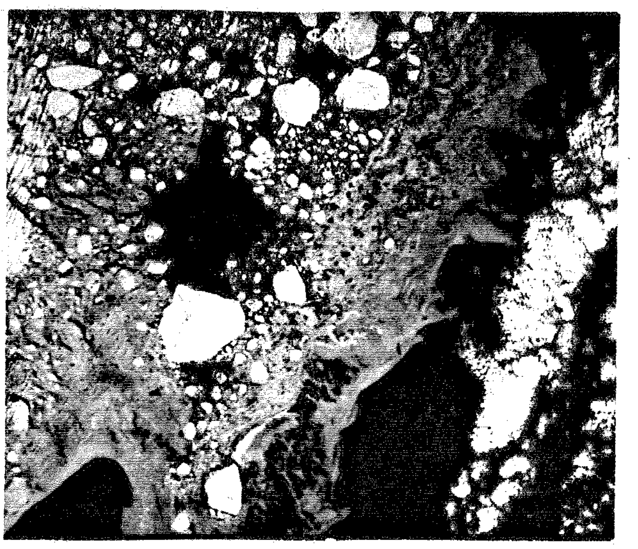

FIG. 7

FIG. 8a

FIG. 8b

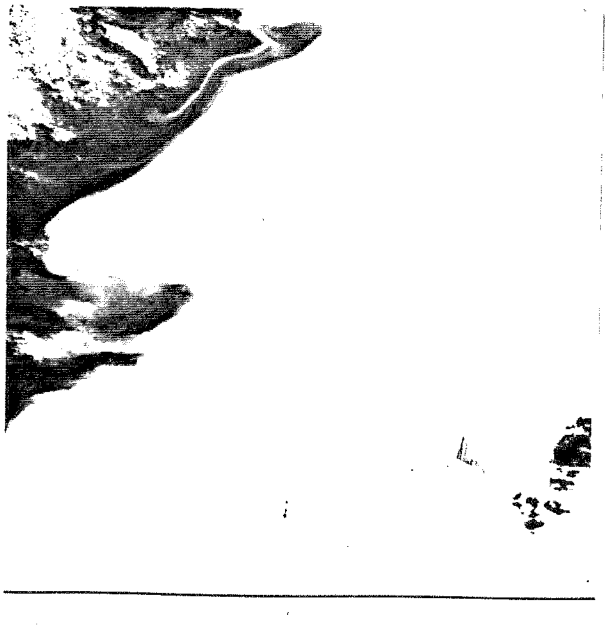

FIG. 8c

FIG. 8d